THE AMERICAN SOCIETY OF MECHANICAL ENGINEERS
345 E. 47 St., New York, N.Y. 10017

92-GT-81

Effects of Back-Pressure in a Lean Blowout Research Combustor

G. J. STURGESS
Pratt & Whitney
East Hartford, Connecticut

S. P. HENEGHAN, M. D. VANGSNESS and D. R. BALLAL

University of Dayton
Dayton, Ohio

A. L. LESMERISES and D. SHOUSE

Wright Laboratories, Wright-Patterson Air Force Base
Dayton, Ohio

ABSTRACT

Experimental information is presented on the effects of back-pressure on flame-holding in a gaseous fuel research combustor. Data for wall temperatures and static pressures are used to infer behavior of the major recirculation zones, as a supplement to some velocity and temperature profile measurements using LDV and CARS systems. Observations of flame behavior are also included. Lean blowout is improved by exit blockage, with strongest sensitivity at high combustor loadings. It is concluded that exit blockage exerts its influence through effects on the jet and recirculation zone shear layers.

INTRODUCTION

Combustion stability is extremely important in gas turbine engines for aircraft use. It is becoming more difficult to ensure that adequate stability margins can be maintained because of current design trends toward airblast atomization of liquid fuel, high temperature rise, and low emissions combustors.

As part of a comprehensive research program to investigate, understand and model lean blowouts in the combustors of aircraft gas turbine engines (Sturgess et al., 1991a), three combustors are utilized. These vehicles consist of a research combustor, a technology combustor, and a generic gas turbine combustor, that reflect the three-phase approach to the problem. The purpose of the research combustor is to yield fundamental information on the lean blowout process to assist in understanding the events taking place in blowout, and so guide in modeling them.

In gas turbine combustor design, it is generally recognized that the end of the flame-holding primary zone is determined by the transverse combustion air jets entering through the combustor liners (Lefebvre, 1983). For combustors using either pure airblast, or hybrid pressure-atomizing primary/airblast secondary fuel injectors, it has been observed that dynamic interactions can occur between the axially-directed jets of atomized fuel/air mixture from the injectors, and these transverse combustion air jets. Recirculation zones of the "external" (Gupta et al., 1984) or "inside-out" type (Sturgess et al., 1990) seem to be especially prone to this behavior. The interaction can be exacerbated if the airflow through the combustor dome (including the injectors) is a significant proportion of the combustor total flow, and if the transverse air jets are close to the dome.

It was therefore felt that the important back-pressure effect exerted on the flame through the presence of the combustion air jets should be included in any simulation of a gas turbine combustor primary zone.

In the research combustor, which was intended for the study of the breakdown of flame stabilization in the primary zone, the essential features of a typical primary zone of modern combustors were reproduced in simplified form (Sturgess et al., 1990). Combustion air jets were not included directly due to the complication involved: however, the back-pressure of these jets was represented by means of exit blockage from the combustor.

RESEARCH COMBUSTOR

The research combustor consists of a central fuel jet of gaseous propane surrounded by an unheated co-axial air jet, with the confluence of the jets centrally located in a nominally circular cross-section duct (Sturgess et al., 1991b). The duct is closed at its forward end to give a backward-facing step. The combustor exit is open to the atmosphere; low pressure effects on lean blowout are simulated by means of dilution through injection of excess nitrogen into the air supply (Sturgess et al., 1991c). The combustor is mounted vertically on an airflow-conditioning unit, that traverses through a cut-out in a fixed optical bench, Figure 1.

Presented at the International Gas Turbine and Aeroengine Congress and Exposition
Cologne, Germany June 1-4, 1992
This paper has been accepted for publication in the Transactions of the ASME
Discussion of it will be accepted at ASME Headquarters until September 30, 1992

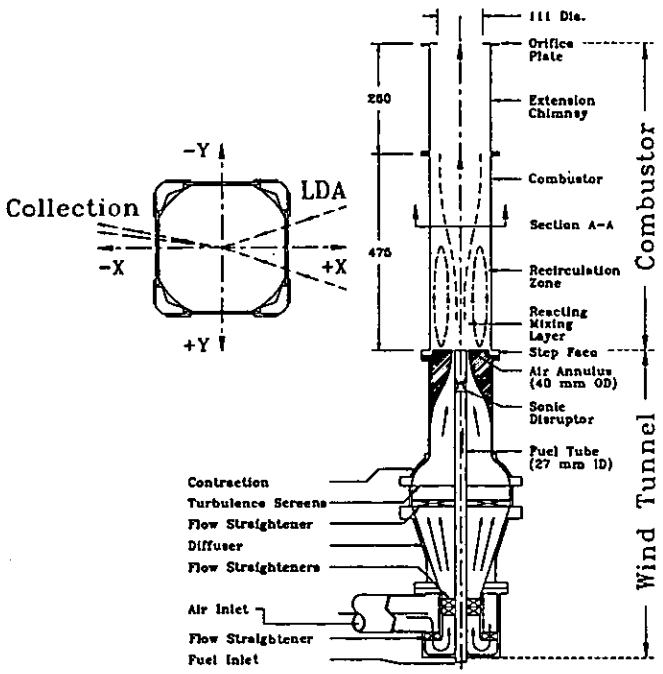

Fig. 1 Research Combustor, Showing Axes Convention

The combustion tunnel was designed and constructed in two sections – a fixed upstream window section providing optical access as needed, and a replaceable downstream chimney. The chimney is available in two lengths, and the combustor can be run with either of these, or with no chimney at all. The combustor has a hydraulic diameter of 150 mm, giving length to diameter (L/D) ratios of 3.167, 4.9 and 6.513 respectively, depending on the chimney arrangement. The inner diameter of the fuel tube is 29.97 mm with a 2-degree half-angle taper over 120mm of its length, and the outer diameter of the air passage at discharge is 40 mm.

Provision is made for exit blockage. The geometric values of exit blockage are 21.0, 45.1 and 62.0 percent of the combustion cross-section. These blockages are achieved by means of thin orifice plates. For the 45.1 percent geometric blockage, "top-hat" exits with tailpipe length to diameter (L/D) values of 1.0 and 2.1 respectively, are also available.

The optical windows can be replaced by metal plates containing arrays of thermocouples for wall temperature measurements, and tappings for static pressure measurements. The combustor may be run with any combination of windows and plates.

LDA ARRANGEMENT

Mean and fluctuating velocity component measurements are obtained by means of a laser-Döppler anemometer (LDA) system (Sturgess et al., 1991b), using 10-degrees off-axis forward scattering. The effective probe volume is 50 x 300 x 750 μm.

The combustor is mounted vertically in the facility (Sturgess et al., 1990), and its centerline constitutes the z-axis, with zero taken as the plane of the step. The x- and y-axes are diametral to the combustor cross-section, with the x-axis aligned with the LDA axis. Velocities parallel to and increasing in the direction of the z-axis, and velocities normal to and directed away from this axis, are also considered positive.

The effective optical window within which data may be taken is defined by: $-68.7 < x < +68.7$ mm, and $-22 < y < 33$ mm; in the downstream direction it is $+2 < z < 358$ mm. This window permits reasonable access to the major flow field features (Sturgess et al., 1991b)

For error assessments, see Sturgess et al. (1991b).

CARS ARRANGEMENT

The laser source for the coherent anti-Stokes Raman Spectroscopy (CARS) optics is a Nd:YAG pulse laser with 10 ns time resolution. The frequency-doubled source green beam (532 nm) is equally divided into four parts; two of these serving as pump beams, while the remaining two pump a dye laser oscillator and amplifier. The dye laser is tuned to provide a red broad-band Stokes beam (110 FWIIM) centered at 607 nm. The red Stokes beam and the two green pump beams are then focused together by a 25 cm focal length lens in a BOXCARS configuration. A 25 x 250 μm measuring spot size is achieved. The CARS signal is collected by a Spex 1702 spectrometer, 1024-element DARSS camera, and Tracor-Northern multichannel analyzer (Figure 2). The raw data are processed by a MODCOMP minicomputer.

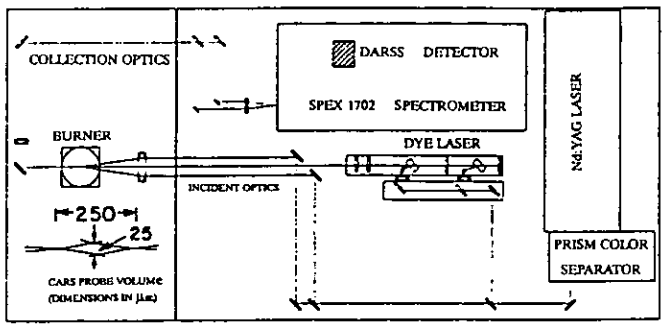

Fig. 2 Arrangement of the CARS System Optics

From the raw data the temperatures are determined by comparing the actual nitrogen spectra to the calculated spectra, using a least-squares fit. The calculation of a nitrogen CARS spectrum requires knowledge of the instrument slit function. Error problems associated with the assumption of a constant slit function when the optical path contains density and/or temperature gradients are avoided by use of a simple method of determining slit functions from the collected data at actual temperature and turbulence levels, by applying local thermodynamic equilibrium principles (Heneghan et al., 1991). This method has been shown to yield improvements in the precision of the CARS measurement (Heneghan and Vangsness., 1991).

Both fuel and air flows were monitored by separate electronic flow control units to within ±0.5 percent and ±1.5 percent respectively. The combined error produced an uncertainty of ±1.5 percent in equivalence ratio, or ±30K in

temperature. Usually, 500 samples were taken for each CARS measurement to ensure that the error in RMS temperature was less than 10K. The RMS temperature is susceptible to CARS instrument noise (Heneghan and Vangsness, 1990). However, in combusting flow the temperature fluctuations are much greater than the instrument noise, and thus the measurement precision (reproducibility) is good. It is estimated overall, that the CARS mean temperature measurement accuracy is within 50K, while the precision is well within 20K. Unlike the LDA, CARS temperature measurements are time-averaged without density-biasing effects.

ISOTHERMAL FLOW FIELD

Development of the isothermal flow field in the research combustor with a free outlet is fully discussed in Sturgess et al. (1991b). Briefly, at a simulated blowout condition, the annular air jet immediately entrains the central fuel jet, generating a small central recirculation bubble of length 17 mm with a beginning about 15 mm downstream of the jet confluence. The individual jets thus quickly merge as they expand into the combustor, and soon lose their identities. This merging is complete by 138 mm from the step. The step generates a large recirculation zone of axial length 7.7 step heights, and with vortex centers about 3.1 step heights downstream.

The addition of exit blockage by orifice plate exerts an obvious effect on the radial profiles of mean axial velocity as the flow accelerates along the combustor centerline to form a vena contracta in the exit plane, with a toroidal recirculation zone forming on the forward face of the orifice plate. For the 4.9 L/D combustor the near-field is unaffected, but the centerline flow acceleration is evident as close as 125 mm downstream from the step-plane. Figures 3 and 4 demonstrate this at 125 and 300 mm stations respectively, for 45.1 percent blockage. Note that the acceleration effect is ameliorated to some extent by the expansion of the combined jets into the combustor.

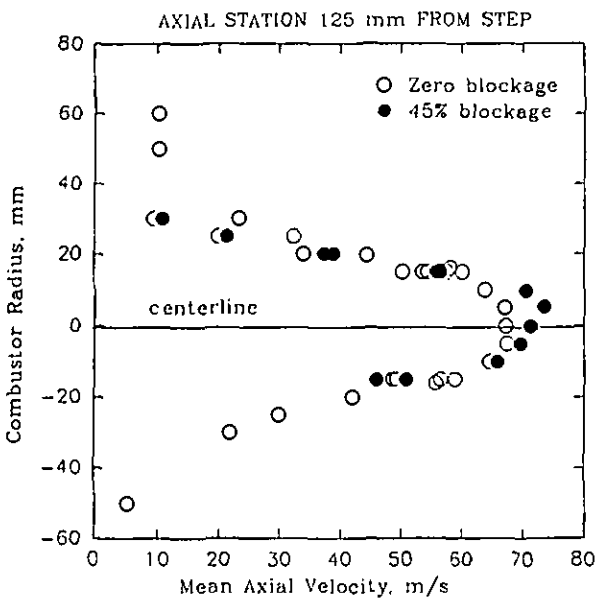

Fig. 3 Radial Profiles of Mean Axial Velocity in Isothermal Flow at 125 mm Downstream from the Step-Plane, Showing Central Flow Net Acceleration with Exit Blockage

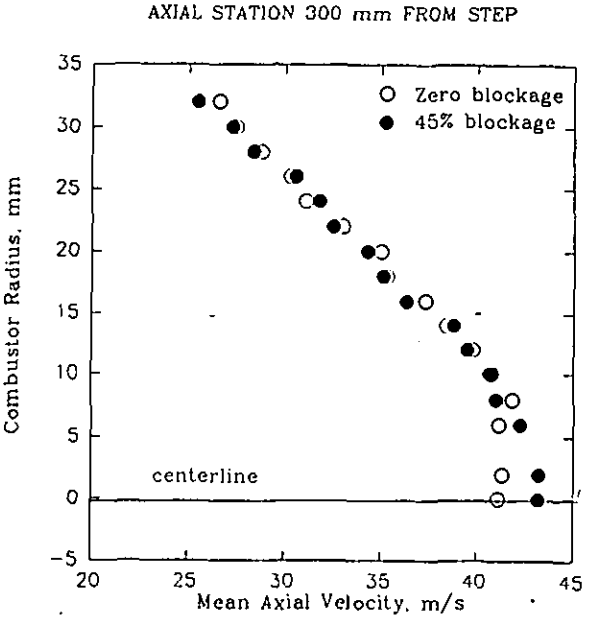

Fig. 4 Radial Profiles of Mean Axial Velocity in Isothermal Flow at 300 mm Downstream from the Step-Plane, Showing Central Flow Net Acceleration with Exit Blockage

There were no changes apparent in the fluctuating velocities with the addition of exit blockage.

The flow field with reaction present is the process of being measured. The features described under isothermal conditions are unchanged in character by the heat release.

EFFECTS OF BLOCKAGE ON FLAME BEHAVIOR

The research combustor operates with three basic flame conditions, depending on the equivalence ratio. For $\phi > 1.05$ approximately, a thin, sheath-like pilot flame is anchored close to the step near the outer diameter of the air passage (Sturgess et al., 1991c). The fuel source for this pilot flame is the step recirculation zone. The major heat release is then precipitated downstream in more or less distributed fashion, by the action of this pilot. Downstream flame-holding takes place in the shear layers associated with the central and step recirculation zones (Sturgess et al., 1991b). For $\phi < 1.05$ approximately, the pilot flame is highly intermittent (Roquemore et al., 1991), and the main flame is lifted (Sturgess et al, 1991c), allowing considerable premixing of reactants to take place prior to combustion. The lifted flame is positioned between 160 to 300 mm from the step-plane. When ϕ reaches 1.5 to 2.0 and before a rich blowout, a separated flame condition is again established where the pilot flame is no longer apparent to the eye, but the main flame does not lift in this case. It is located about 30 to 40 mm downstream from the step.

Lean blowout data were correlated on the basis of a combustor loading parameter (Sturgess et al., 1991c), derived from reaction rate theory as,

$$LP = \dot{m}_{Tot} / (VP^{n}F)$$

where for gaseous fuels and with simulation of low pressures by excess nitrogen injection,

$$\dot{m}_{Tot} = \dot{m}_{fuel} + \dot{m}_{air} + \dot{m}_{nitrogen}$$

V = reactor volume

P = effective pressure

n = apparent global reaction order
$= 2\phi / (1 + \dot{m}_{nitrogen} / \dot{m}_{air})$

ϕ = equivalence ratio

F = temperature correction factor (to 400K)
$= 10^{0.00143 T_{in}} / 3.72$

T = inlet temperature of reactants in K.

Use of LP for blowout correlations follows from the adoption of a stirred reactor modeling approach (Sturgess et al., 1991a). It also forms a useful way of characterizing the degree of "flame straining" present in the combustor.

Figure 5 provides a map of flame behavior as a lean blowout is approached, obtained by visual observation. The combustor L/D was 4.9, and the exit was a 45.1 percent blockage orifice plate. Inlet temperatures for the reactants were constant at 293K, and no excess nitrogen was injected. The Reynolds number of the annular air jet was in the range of 24,800 to 46,000. The attached and lifted flame conditions are illustrated in Figure 2 of Sturgess et al. (1991c).

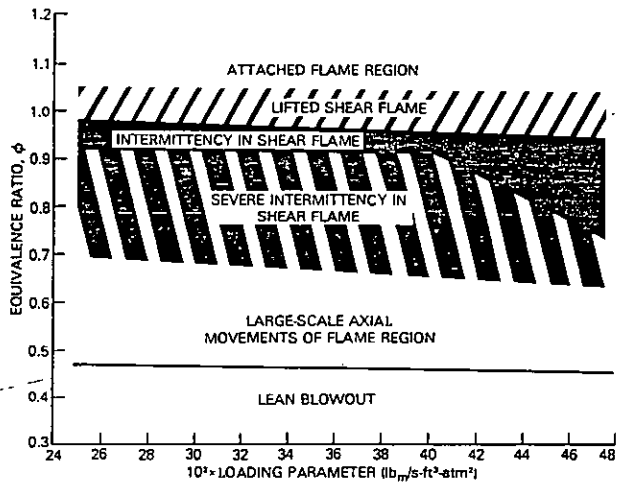

Fig. 5 Flame Behavior as Lean Blowout is Approached at Low Combustor Loadings with 45 Percent Exit Blockage

The range of loading parameter in Figure 5 is such that lean blowouts were obtained close to the flammability limits for propane/air mixtures at ambient conditions (Lewis and von Elbe, 1961). The flame behavior seen is both reversible and repeatable. Flame lift can be seen at about 1.05 equivalence ratio, and is insensitive to loading parameter over the limited range covered. Subsequent tests (Sturgess et al., 1991c) with injection of excess gaseous nitrogen into the air stream showed no effects on equivalence ratio for flame-lift. When the fuel flow was progressively reduced at constant airflow, or the airflow was progressively increased at constant fuel flow, the same sequence of flame events leading to a blowout took place. These events are shown on Figure 5. Eventually, an oscillatory flow situation develops, with large-scale axial movements of the entire lifted flame about a mean position. This motion leads, in due course, to lean blowout.

The existence of the sequence of flame behaviors did not qualitatively change with differences in exit blockage. However, the equivalence ratio for flame lift was observed to decrease slightly with increase in blockage due to orifice plates (Figure 6). Similar behavior was observed with increase in tailpipe L/D for the 45.1 percent blockage top-hat section (Figure 7).

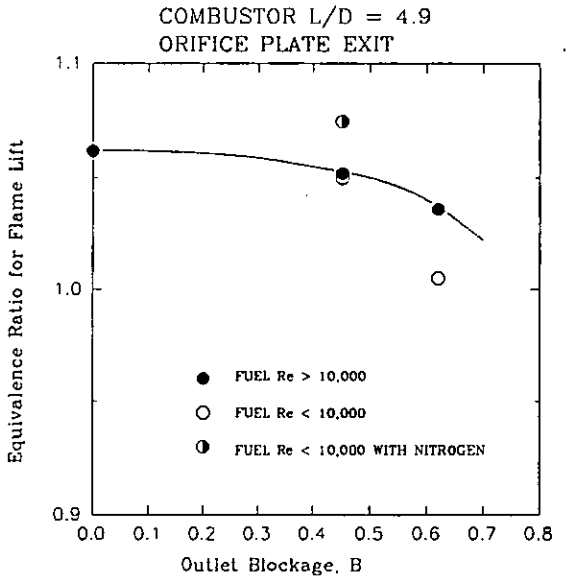

Fig. 6 Dependence of Equivalence Ratio for Flame Lift on Exit Blockage for Low and Intermediate Combustor Loadings

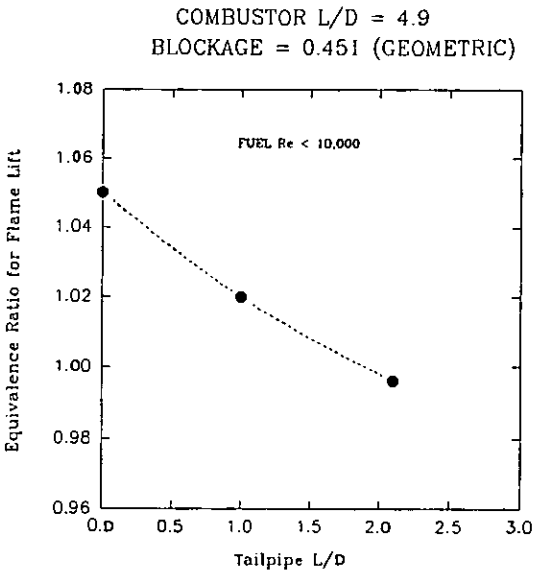

Fig. 7 Dependence of Equivalence Ratio for Flame Lift on Tailpipe Length for 45 Percent Geometric Exit Blockage

The significance of the 10,000 Reynolds number for the fuel jet in Figures 6 and 7 is that this value represents a critical threshold for transition to turbulent flow for propane (Lewis and von Elbe, 1961).

A fairly strong influence on the equivalence ratio for the onset of the large-scale axial oscillation of the lifted flame was observed, as shown in Figure 8. Increased blockage raises this equivalence ratio and is therefore destabilizing, opposite to the effect on flame lift. Note the significance of air jet Reynolds number.

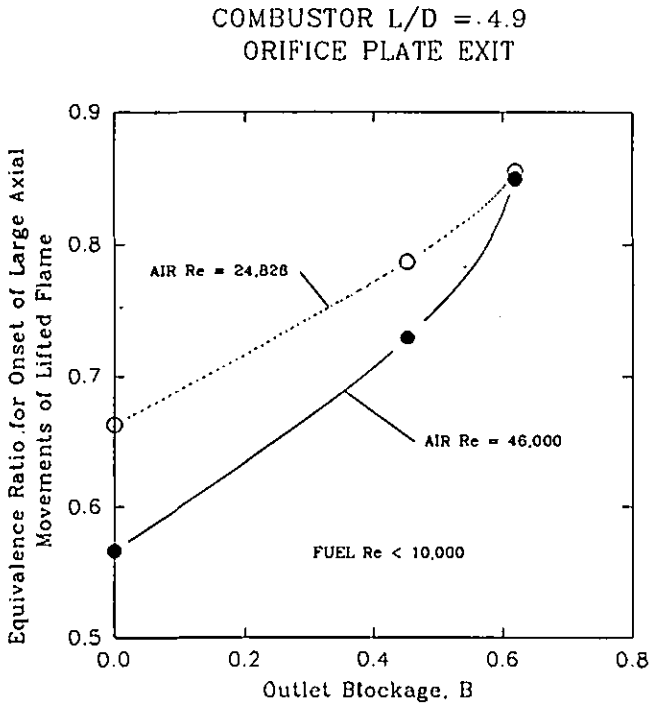

Fig. 8 Influence of Exit Blockage and Combustor Loading on Equivalence Ratio for Onset of Axial Movements of the Lifted Flame

It is apparent that the loss of the important pilot flame marks the beginning of a lean blowout sequence. A similar importance of the pilot flame is observed as a rich blowout is approached. Figure 9 shows the dependence of rich equivalence ratio for loss of the pilot flame (to result in a separated main flame), on exit blockage in the 4.9 L/D combustor. Note that on the rich-side, decreasing equivalence ratio denotes a maximum loss of stability at 45.1 percent blockage. At given blockage this rich equivalence ratio for pilot flame loss decreases as the combustor loading is increased; Figure 10 demonstrates this for the 4.9 L/D combustor at 45.1 percent exit blockage by orifice plate.

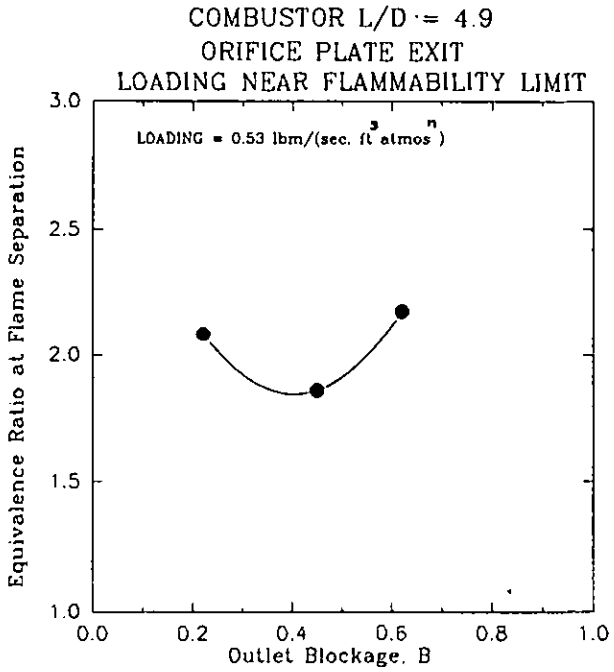

Fig. 9 Dependence of Equivalence Ratio for Flame Separation on Exit Blockage for Low Combustor Loading

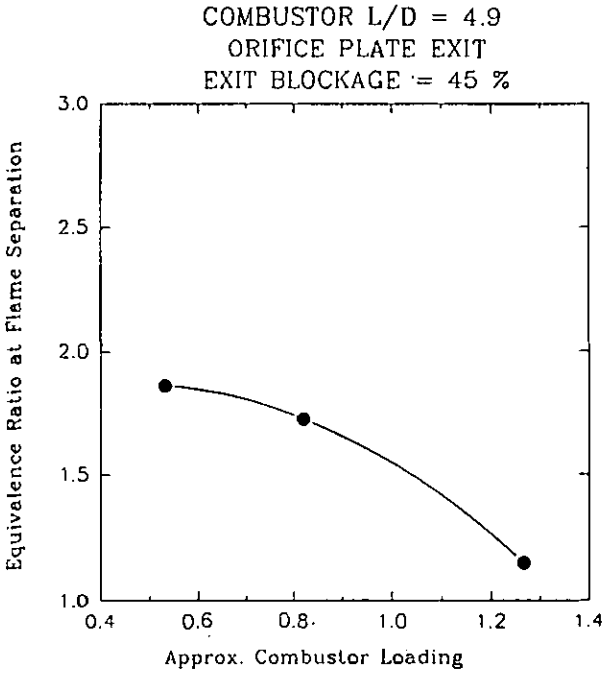

Fig. 10 Influence of Combustor Loading on Equivalence Ratio for Flame Separation at 45 Percent Exit Blockage

DIRECT EFFECTS ON LEAN BLOWOUT

It was observed for low values (about 0.18 $lb_m/(sec.ft.^3 atmos.^n)$ close to the flammability limits for propane/air mixtures at these conditions) of the loading parameter that the blowout equivalence ratio decreased linearly as the exit blockage by orifice plate was increased. This is shown in Figure 11, and is somewhat surprising since the lifted flame is positioned (Roquemore et al., 1991) in the regions where the mean flow is beginning to be accelerated due to the blockage (Figures 3 and 4), at least in isothermal flow. Heat release should increase the flow acceleration. The improvement in stability depended on the combustor L/D ratio; for a given blockage, the shorter the combustor the less stable it was and the greater its sensitivity to the exit blockage. For the 4.9 L/D combustor at this loading, the lean blowouts were virtually independent of exit blockage.

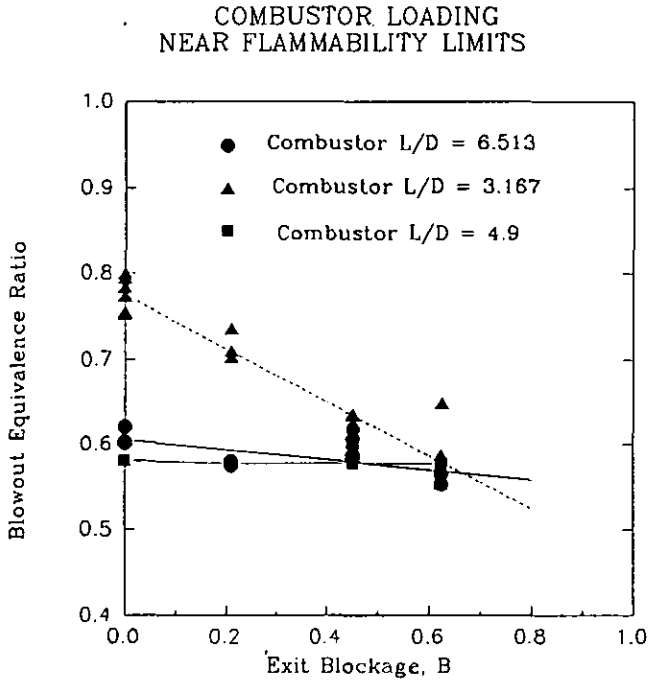

Fig. 11 Influence of Exit Blockage on Lean Blowout at Low Combustor Loading in Three Combustor Lengths

For a fixed exit orifice plate blockage of 45.1 percent at slightly higher loading parameter, the dependency on L/D is given in Figure 12, where it can be seen that an optimum L/D exists. Close to the flammability limits there is also a fairly strong sensitivity of blowout equivalence ratio to combustor loading parameter. The existence of the optimum combustor length for maximum stability close to the flammability limits (Lewis and von Elbe, 1961) can be attributed to the occurrence of acoustic coupling (organ-pipe resonance driving eddy shedding off the step at 55 Hertz) at large L/D (Heneghan et al., 1990), and outlet interference with flame holding at small L/D.

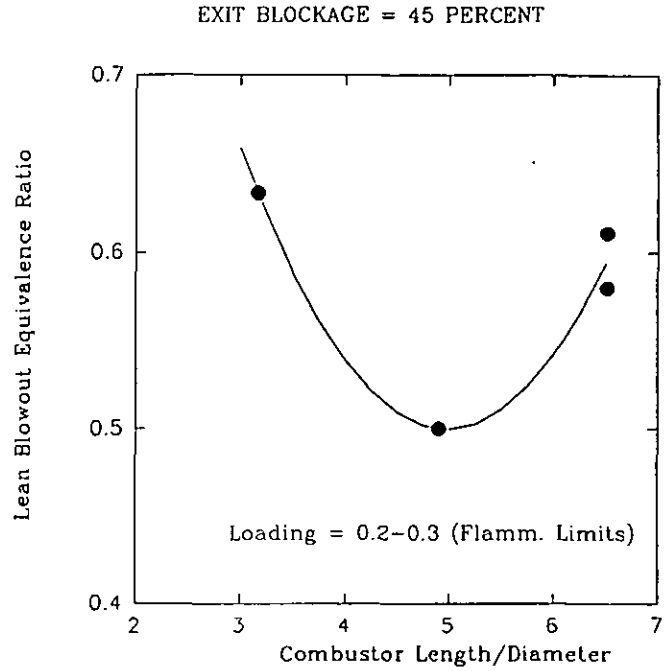

Fig. 12 Dependence of Lean Blowout at Low Loadings on Combustor Length with 45 Percent Exit Blockage

At 45.1 percent exit blockage the peak amplitude of the 55 Hz frequency signal measured inside the combustor by Kistler pressure transducers, was increased by a factor of 5.5 when the combustor L/D was increased from 3.167 to 6.513. For the 4.9 L/D combustor with 45.1 percent exit blockage (and the acoustic treatment described in Heneghan et al., 1990), the peak-to-peak amplitudes for low frequency oscillations (1-600 Hz) were less than 0.69 N/m^2 and for high frequency oscillations (1-5 KHz) the amplitudes were less than 6.9 N/m^2.

Figure 13 displays the sensitivity to exit blockage in the 4.9 L/D combustor operating at loadings (10 $lb_m/(sec.ft.^3 atmos.^n)$) near to the peak heat release rate condition (obtained with a combination of high airflow rates and injection of excess nitrogen as a diluent). Again, the blowout equivalence ratio decreases linearly with increasing blockage. However, when contrasted with the sensitivity to blockage for this combustor near the flammability limits (Figure 11), it is seen that blockage exerts a much more powerful influence on stability at this higher loading.

The general conclusion can be drawn that exit blockage improves the lean stability of the research combustor. The effectiveness of blockage in improving the stability in a combustor of given length, depends on the loading at which the combustor is operated. Of the three combustor lengths evaluated (and for operation at low loadings at least), the 4.9 L/D combustor has the best stability at any blockage level between 0 and 62 percent. Exit blockage reduces the rich stability of the research combustor, and the extent of this also depends on the combustor loading.

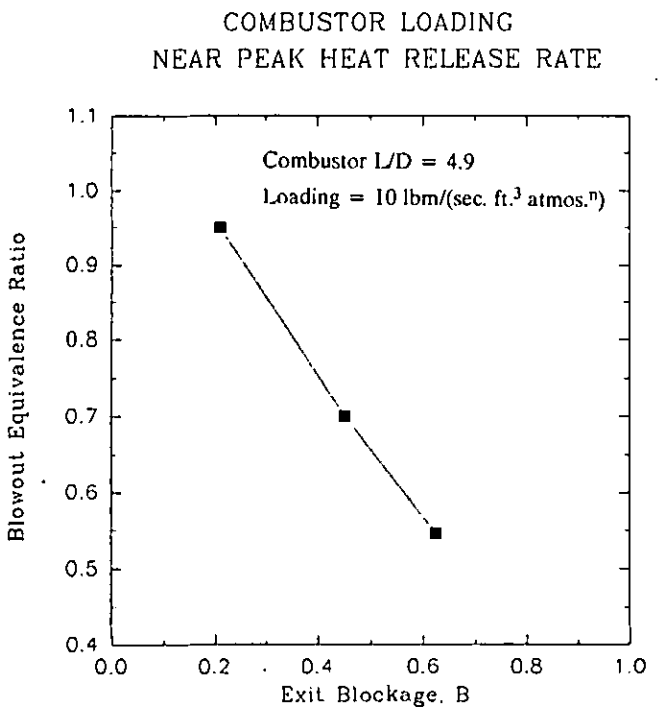

Fig. 13 Influence on Lean Blowout of Exit Blockage at High Combustor Loading

WALL TEMPERATURE BEHAVIOR

The wall temperatures for the combustor are needed to provide boundary condition information for subsequent computational fluid dynamic calculations to be made in attempts to model the lean blowout process. They can also provide by inference, additional information concerning development of major flow features in the combustor.

Wall temperatures are most conveniently expressed in nondimensional form, sometimes known as Metal Temperature Factor (MTF), and defined by,

$$MTF = \frac{T_s - T_{in}}{T_{ad,fl} - T_{in}}$$

where

T_s = wall temperature

$T_{ad,fl}$ = adiabatic flame temperature.

For premixed flames, MTF represents a normalized wall temperature, and is particularly useful in the present case therefore, because of the partial premixing that takes place when the flame is lifted.

Figure 14 compares at 44.5 mm downstream from the step and inside the step recirculation zone, actual thermocouple temperatures over a range of equivalence ratios against temperatures derived from the MTF trend with downstream distance. Data are provided for zero and 45.1 percent exit blockage in the 4.9 L/D combustor. The tests were made for a variety of jet velocity ratios and combustor flow functions. No effect of velocity ratio was apparent, and substantial increase in flow function resulted in only a negligible increase in MTF.

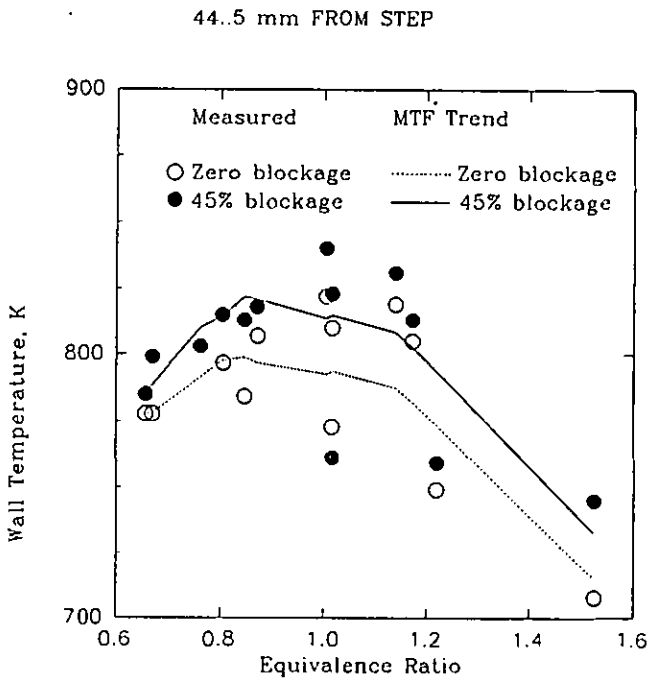

Fig. 14 Comparison of Actual Wall Temperatures with Smoothed Values Over a Range of Equivalence Ratios, Showing Influence of Exit Blockage

The figure shows that wall temperatures in the recirculation zone increase with combustor exit blockage by about 20 to 25 deg. K for 45.1 blockage. Peak temperatures occur at equivalence ratios in the range of 0.9 to 1.1. For the attached flame condition ($\phi \geq 1.05$), temperature levels are about 820K, and fall to about 780K as lean blowout is approached.

The form of MTF variation with equivalence ratio is shown in Figure 15 for a station 146 mm downstream from the step (still inside the recirculation zone). The behavior in the figure is typical of all axial stations along the combustor. MTF decreases with increasing equivalence ratio up to an equivalence ratio of about 0.95, and then becomes independent out to a value of 1.6. There is negligible effect of blockage on MTF at this station.

The "break" in the curve of Figure 15 may be interpreted as representing the flame-lift condition. The inferred equivalence ratios for flame-lift based on this break for different axial locations are shown in Figure 16 compared with the equivalence ratios for flame-lift based on direct observation (Figure 6). As might be anticipated, inferences based on data from downstream are in better agreement with direct observations. No effect of blockage is apparent on the inferred flame-lift, which does not conflict with direct observation in Figure 6.

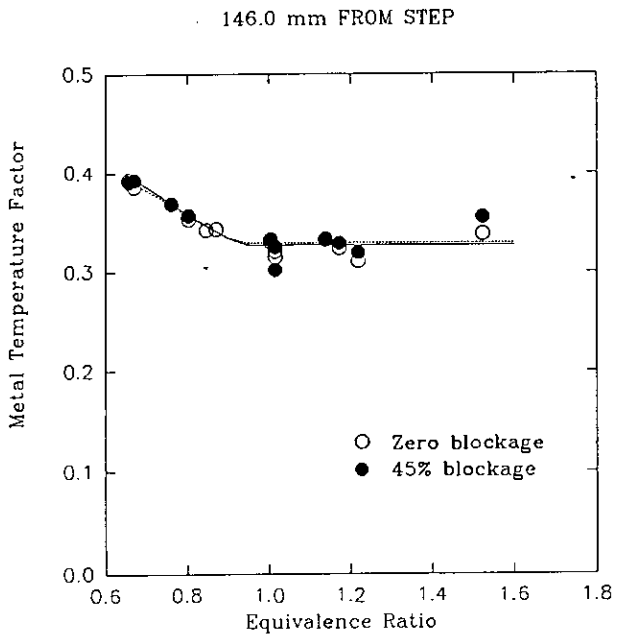

Fig. 15 Normalized Wall Temperatures at 126 mm from Step–Plane for Zero and 45 Percent Exit Blockage, Showing Influence of Equivalence Ratio

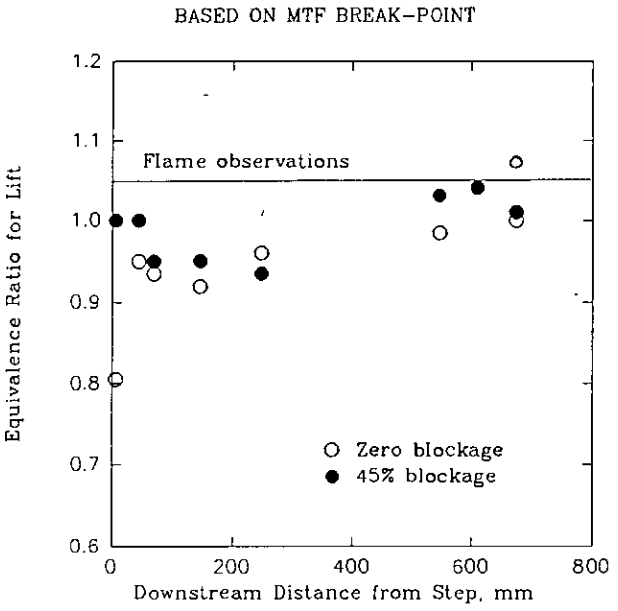

Fig. 16 Indicated Equivalence Ratios for Flame–Lift from Wall Temperatures, Compared with Direct Observations

The variations of the maximum value of MTF with equivalence ratio for 0, 45.1 and 62 percent geometric blockages are given in Figure 17; the flame condition – lifted or attached – is delineated based on Figure 6. The values of maximum MTF, and the positions at which they occur, were derived at each equivalence ratio from differentiation of curve fits to MTF versus axial distance information obtained from the curves in plots such as given in Figure 15.

Figure 17 indicates that maximum MTF reaches its minimum value at about the equivalence ratio for flame–lift. Exit blockage does not affect the value of maximum MTF, but maximum MTF does increase as lean blowout is approached.

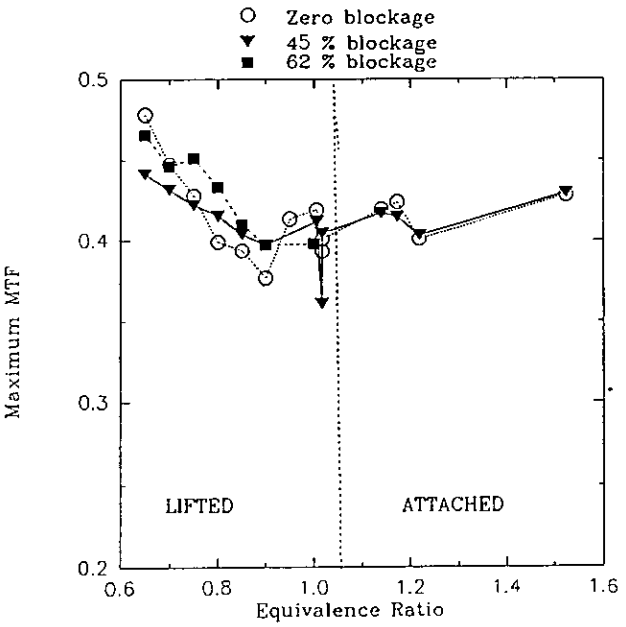

Fig. 17 Variations of Maximum Normalized Wall Temperatures for Lifted and Attached Flames at Several Values of Exit Blockage

When the position at which maximum MTF is reached is plotted in similar fashion in Figure 18, a strong effect of blockage is apparent for lifted flames; equivalence ratios for attached flames do not influence this position significantly. For the three blockages shown, the position of maximum MTF is roughly constant around 450 mm from the step for attached flames.

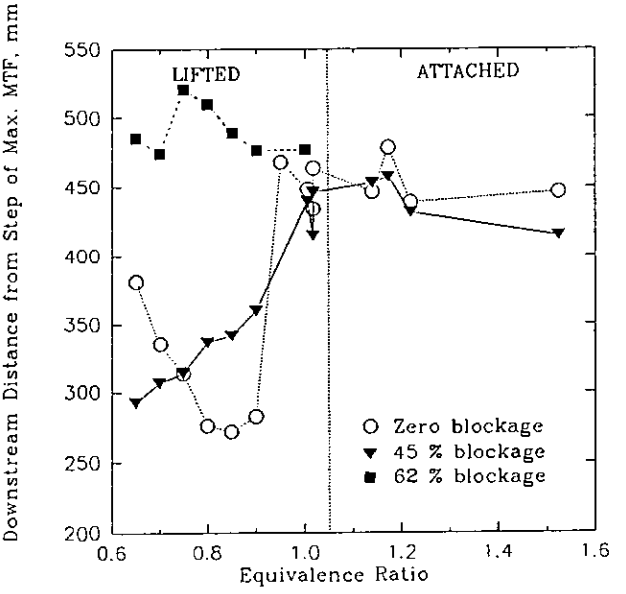

Fig. 18 Dependency of Position of Maximum Normalized Wall Temperature on Exit Blockage for Lifted and Attached Flames

When equivalence ratio is reduced so that a lifted flame is established, an unrestricted combustor exit results in the position of maximum MTF initially moving back toward the step. However, for an equivalence ratio of 0.9, the closest position to the step is reached at about 270 mm; therefore, as equivalence ratio is further lowered toward a lean blowout, the position again moves downstream as the flame-lift increases.

The addition of exit blockage introduces an additional recirculation zone (on the orifice plate upstream face) into the combustor, and the existence of this recirculation is how blockage exerts an influence on the position of maximum MTF. The position of maximum MTF is associated with the reattachment plane of the step recirculation zone since this is where the jet shear layers reach the combustor wall (Sturgess et al., 1991b). These jet shear layers are where the majority of the heat release takes place during combustion, whether or not the pilot flame is attached (Sturgess et al., 1991a). Movements of the position of maximum MTF therefore reflect, albeit in crude fashion, movements of the reattachment plane for the step recirculation zone. The lack of blockage-effect on the value of maximum MTF (Figure 17) indicates that heat release in the jet shear layers is not substantially changed by combustor exit blockage; however, the trajectory of these shear layers is (Figure 18), possibly due to flow acceleration as a result of the heat release. The behavior evident in Figure 18 for 45.1 and 62 percent blockage is the result of interactions between the step and orifice plate recirculation zones, due to heat release rate as equivalence ratio is varied, and modified by the two flame conditions.

With this flow model, the lifted-flame (partially premixed) behavior for maximum MTF in Figure 18 at zero exit blockage is consistent with the findings of Morrison et al. (1987), Pitz and Daily (1983), and Stevenson et al. (1982) for premixed flames that a step recirculation zone at fixed (turbulent) Reynolds number decreases in size with increasing equivalence ratio. The minimum distance occurring at an equivalence ratio of 0.9 suggests that pilot flame attachment is becoming evident before the directly-observed equivalence ratio of 1.05 (Figure 6). Examination of the intermittency of the pilot flame (Roquemore et al., 1991, and Chen, 1991) tends to confirm this suggestion.

WALL STATIC PRESSURES

For an atmospheric pressure discharge combustor with exit blockage, wall static pressures provide means for a convenient assessment of the extent of the additional recirculation zone set up on the orifice plate upstream face. With a free exit, the difference between ambient pressure and wall static pressure in the combustor reaches zero in the exit plane. However, when the exit is restricted, this difference reaches zero at some position inside the combustor (Heneghan et al., 1990). The position where this occurs marks the stagnation plane for the aft recirculation zone on the orifice plate.

In isothermal flow the wall static pressure at a given station is a function of the jet velocity ratio λ, and the inlet flow parameter, as can be seen for a station 44.5 mm downstream, in Figure 19. As Figure 20 demonstrates, when exit blockage is introduced, the dependency of wall static pressure on velocity ratio is suppressed. Combustion also suppresses the dependency on jet velocity ratio, even for a free exit. This is illustrated in Figure 21, where it is also shown that the flame condition does not exert an influence.

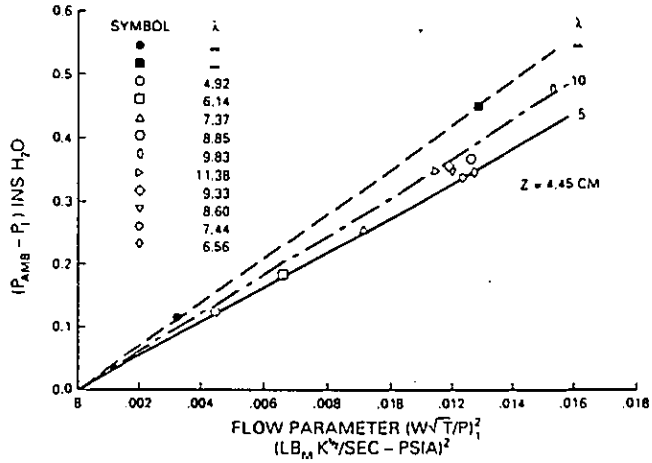

Fig. 19 Dependency of Wall Static Pressures in the Step Recirculation Zone on Inlet Flow Parameter and Jet Velocity Ratio in Isothermal Flow with a Free Exit

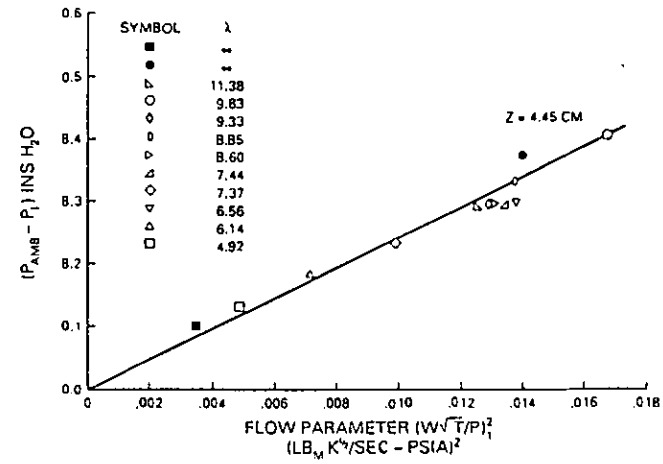

Fig. 20 Suppression of Dependency of Wall Static Pressure on Jet Velocity Ratio by Exit Blockage in Isothermal Flow

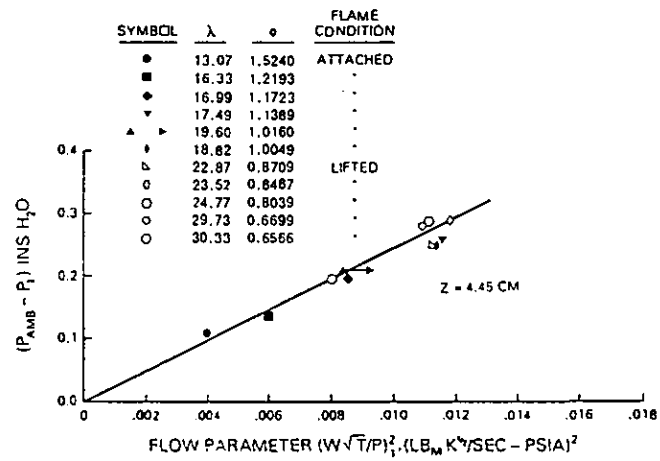

Fig. 21 Suppression of Dependency of Wall Static Pressure on Jet Velocity Ratio by Combustion with a Free Exit

Again using curve fits and differentiation, the axial positions along the combustor at which atmospheric pressure was attained, were found. Typical wall static pressure axial distributions are given in Figure 3 of Heneghan et al. (1990). Figure 22 shows that in isothermal flow this condition was reached at a constant 580 mm approximately, with 45.1 percent exit blockage, and was so regardless of inlet flow parameter or jet velocity ratio. With combustion and the same blockage, the position for atmospheric pressure was a strong function of equivalence ratio, as Figure 23 shows, where the leading-edge of the aft recirculation zone moves progressively forward in the combustor as equivalence ratio is reduced, independent of flame condition.

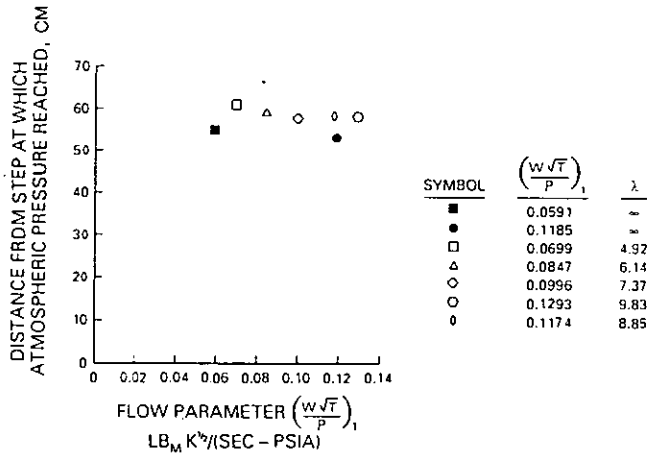

Fig. 22 Independence from Inlet Flow Parameter and Jet Velocity Ratio of Position Where Atmospheric Pressure Is Reached on the Combustor Wall, in Isothermal Flow with 45 Percent Exit Blockage

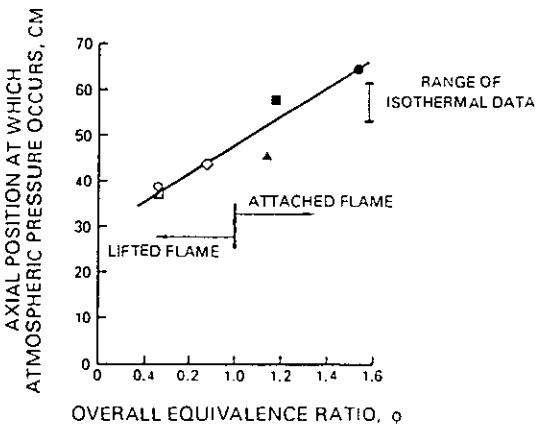

Fig. 23 Variation of Downstream Position Where Wall Static Pressure Reaches Atmospheric with Equivalence Ratio at 45 Percent Exit Blockage

At 62 percent blockage the position at which atmospheric pressure was attained was always greater than 600 mm from the step, and thus could not be accurately determined from the static tap positions available.

RELATIONSHIP BETWEEN RECIRCULATION ZONES

The information on the end of the step recirculation zone inferred from MTF data (Figure 18) can be combined with the information on the beginning of the orifice plate recirculation zone from the static pressure data (Figure 23) in order to examine the relationship between these two important flow features in the restricted-exit combustor.

Figure 24 shows a combination of Figures 18 and 23 for 45.1 percent exit blockage with combusting flow. It can be deduced that there is always positive separation between the end of the step recirculation zone and the beginning of the orifice plate recirculation zone for this blockage. Furthermore, for lifted flames, this separation is maintained at a constant distance of about 80 mm, so that direct interference never happens. For attached flames, the separation distance increases, as Figure 25 shows.

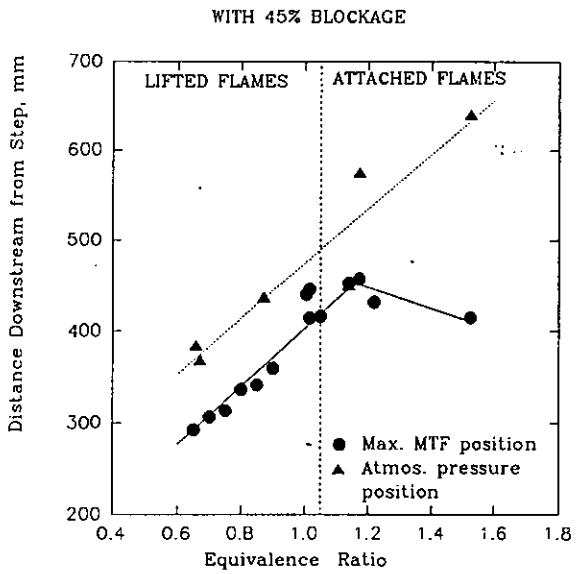

Fig. 24 Downstream Positions Where Atmospheric Pressure and Maximum Normalized Wall Temperature Are Attained as Equivalence Ratio Is Varied for Fixed Exit Blockage

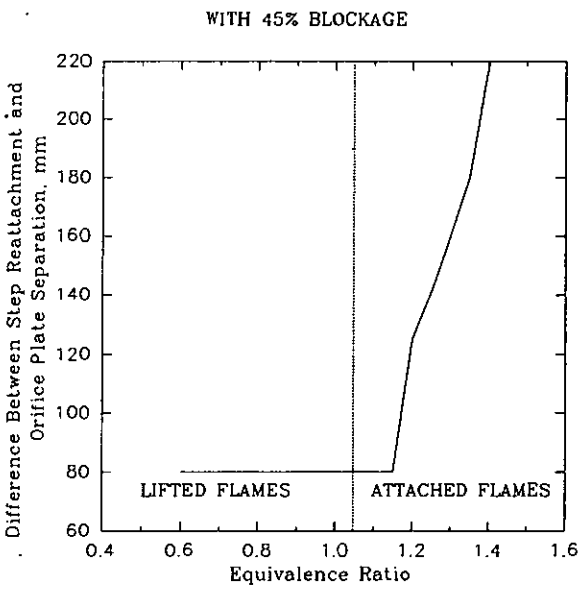

Fig. 25 Distance Between Recirculation Zones for Lifted and Attached Flames at Fixed Exit Blockage

For 62 percent blockage, it appears as though direct interference between zones does not occur either, despite the inferred position of the end of the step recirculation zone being further downstream at around 500 mm for all equivalence ratios (Figure 18).

GAS TEMPERATURE PROFILES

Limited gas temperature measurements were made using the CARS system. Profiles along the combustor centerline and, radially, close to the step, were taken at 0, 45.1 and 62 percent exit blockage by orifice plates in order to assess what blockage did to the all-important step recirculation zone. This was a quick preliminary look made prior to more extensive field-mapping of temperature to be reported separately.

The axial profiles of mean temperature along the combustor centerline at 45.1 percent exit blockage for lifted and attached flames are given in Figure 26, where the temperatures are presented as the ratio of actual temperature to the adiabatic flame temperature. The combustor loadings in both cases are in the range of 0.7 to 0.76 $lb_m/(sec.ft.^3atmos.^n)$, i.e., fairly near to the lean flammability limit. For both flames the temperature initially falls, and then increases again for distances greater than 100 mm from the step-plane. By consideration of Sturgess et al. (1991b), the increases in centerline mean temperature can be associated with the inner edge of the reacting jets shear layer reaching the centerline and thereby introducing sufficient oxidant for extensive chemical reaction to take place on the centerline. The initial distance in this profile can therefore be viewed as a conditional thermo-chemical potential core region. Note that the position of mean temperature increase is in the region where in isothermal flow the centerline mean axial velocity begins to accelerate with the 45.1 percent exit blockage (Figure 3). Also, for the attached flame the dimensionless mean temperature level is generally increased over that for the lifted flame.

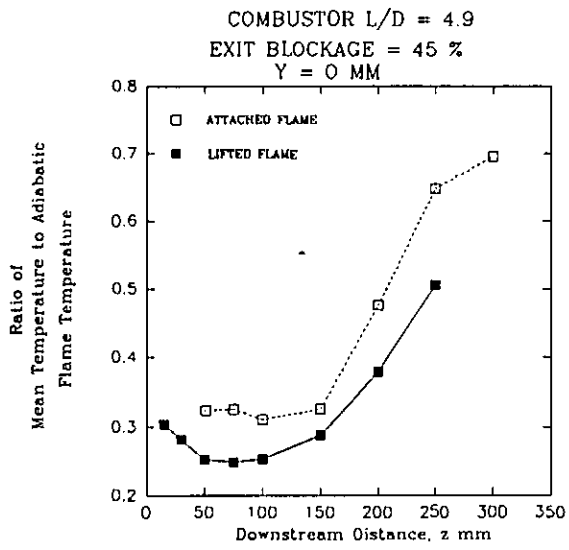

Fig. 26 Centerline Profiles of Dimensionless Mean Gas Temperature for Attached and Lifted Flames at Fixed Exit Blockage

Radial profiles of dimensionless mean temperature for the condition above are given in Figure 27 for a downstream station 5 mm from the step. Comparison of these profiles reveals the effect of the attached flame on mean temperature, and shows the pilot flame to be located at a radius of 17 to 20 mm. The probability distribution functions (p.d.f.) confirm this definition. This is somewhat consistent with the mean position of 24 mm radius for the attached flame determined at 10 mm downstream with thin filament pyrometry (TFP) (Roquemore et al., 1991). Again, the levels of dimensionless temperature are higher at all radial positions for the attached flame condition. The p.d.f.'s for the lifted flame condition agree with the measurements of the spontaneous OH emission given in Roquemore et al. (1991), that there is a finite probability of the pilot flame being present part of the time, even though the main flame is fully lifted and an anchored pilot flame is not directly observed. For both lifted and attached flames, the step recirculation zone provides a significant high-temperature reservoir for the combustion processes developing in the shear layers.

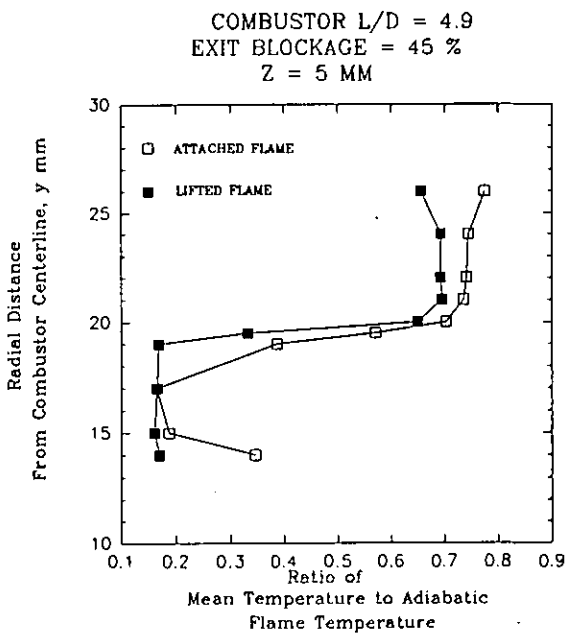

Fig. 27 Radial Profiles of Dimensionless Mean Gas Temperature in the Step Region for Attached and Lifted Flames at Fixed Exit Blockage

Note that both Figures 26 and 27 indicate an elevation of gas temperatures over the inlet conditions close to the confluence of the jets and around the region encompassing the small, central recirculation bubble (Sturgess et al., 1991b). Although not yet supported by strong direct evidence, it has been hypothesized (Sturgess et al., 1991a) that nonstationary flow interactions of the fuel and air jets with the central recirculation bubble result in additional radial mass transport of reactants. Such mass transport could account for early chemical reaction and hence, the observed elevated temperatures close to the orifice. The p.d.f. at a radius of 14 mm for an equivalence ratio of 1.36 at a combustor loading of 0.428 $lb_m/(sec.ft.^3atmos.^n)$ shows that there is an equal probability of the flame being present as there is of fluid at

inlet temperatures. This radius marks the position of the outer-edge of the fuel tube. For this temperature condition to be so, either direct flame or a hot gas ignition source from the step recirculation zone must be transported completely across the annular air-jet path (see Figure 1).

The addition of blockage increases the centerline mean temperatures for lifted flames at loadings fairly near to the lean flammability limit. The effect is particularly strong for distances closer to the confluence of the jets than 100 mm, as Figure 28 shows. The radial profiles of dimensionless mean temperature indicate that blockage slightly increases the temperature in the step recirculation zone.

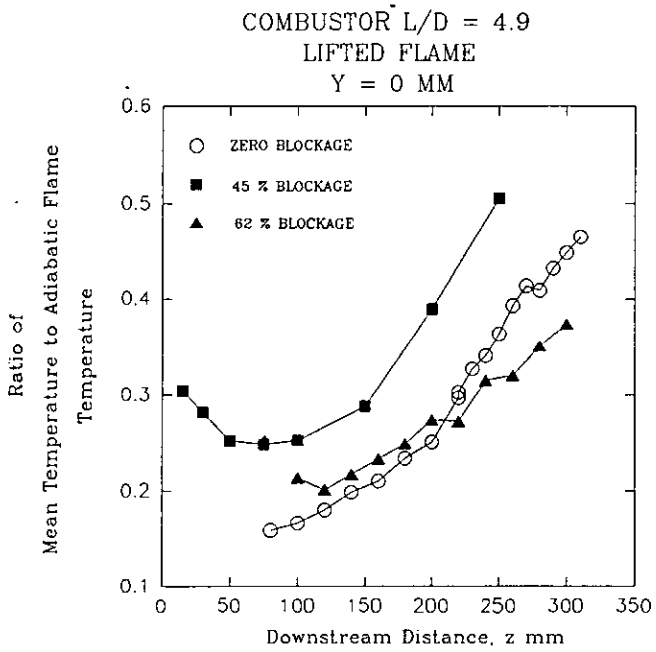

Fig. 28 Comparison of Centerline Profiles of Dimensionless Mean Gas Temperatures for Lifted Flames at Various Exit Blockages

The centerline profiles of the ratio of the RMS value of fluctuating temperature to mean temperature for 0, 45.1 and 62 percent exit blockage in the 4.9 L/D combustor are given in Figure 29. The equivalence ratios are such that the flames were all lifted, and the combustor loadings were 0.7 to 0.76 $lb_m/(sec.ft.^3 atmos.^n)$. The fluctuating temperatures superimposed on the mean temperatures are not significantly affected by exit blockage. What is noteworthy, however, is the dramatic increase in the fluctuating component for distances closer than 50 mm to the jet origins. This is associated in particular with the forward stagnation point of the small, central recirculation zone, which for isothermal flow is situated at about 14 mm from the origin.

Figure 30 presents radial profiles of the ratio of RMS temperature to mean temperature at 5 mm downstream from the step-plane for a range of exit blockage at the same operating conditions as for the previous figure, i.e., lifted flame at light loadings. Temperature fluctuations in the step recirculation zone are not much affected by the exit blockage. In sharp contrast, the existence of any blockage at all exerts a powerful suppressing effect on fluctuations in the jet shear layers.

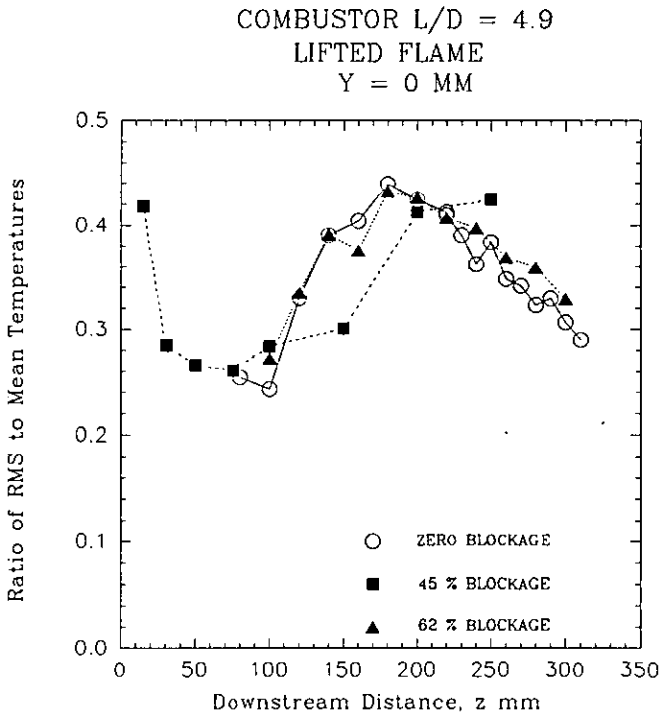

Fig. 29 Comparison of Centerline Profiles of Dimensionless Fluctuating Gas Temperatures for Lifted Flames at Various Exit Blockages

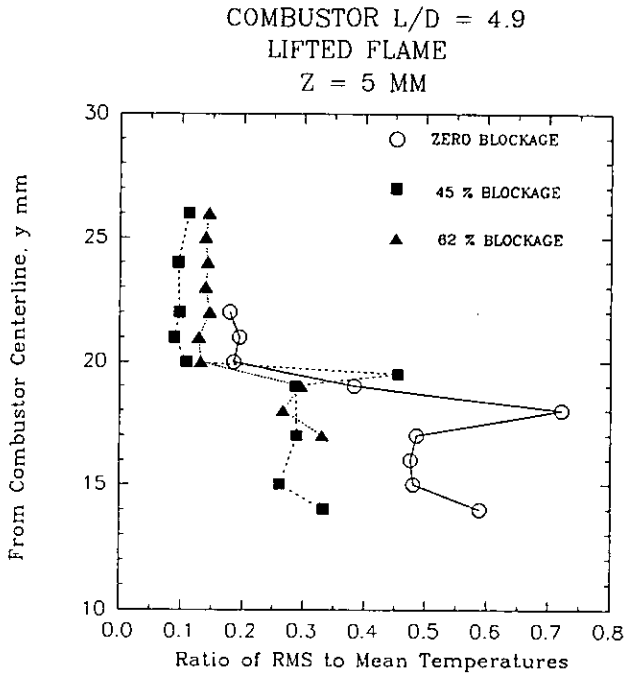

Fig. 30 Radial Profiles of Dimensionless Fluctuating Gas Temperatures in the Step Region for Lifted Flames at Various Exit Blockages

Whether the flame is lifted or attached, there are no changes in temperature fluctuations in the step recirculation zone at 5 mm downstream with 45.1 percent exit blockage. There appear to be some differences for the two flame conditions in the shear layers (possibly the pilot flame), but the present data are not sufficient to be sure.

DISCUSSION

The long-term intent for the research program, of which this effort is but a part, is to derive calculation procedures for lean blowout in gas turbine engine combustors. One of the calculation procedures being developed for this purpose is computational fluid dynamics (CFD). For viability, CFD should be able to provide a reasonable simulation of the real physical behavior involved in the lean blowout process. It is therefore required that significant flame events in the blowout process should be experimentally identified and characterized. The attached, separated and lifted flames and the influence of combustor geometry on the operational conditions under which these are encountered, hence form a significant part of the data base. The ability to calculate these characteristics will form a critical test of the efficacy of any CFD modeling of lean blowout.

The research combustor exhibits a distinct and repeatable flame pattern change as it blows out on the lean side (Figure 5). There are similarities in the flame changes for both rich and lean blowouts. A key element in these sequences of flame change is the loss of the thin, sheath-like pilot flame anchored at the outer diameter of the air jet. This pilot flame serves as a continuous ignition source for the main flame that then originates in the shear layers associated with the fuel and air jets, and the recirculation zones. For rich blowouts, loss of the pilot flame does not result in obvious changes in the main flame, either in position or character. It tends to remain concentrated in the shear layers. However, for lean blowouts, loss of the pilot flame causes the main flame to lift to a downstream position. This clearly allows significant premixing of reactants to occur, with the result that the main flame in its lifted position is more distributed across the width of the combustor. Blowout in the separated rich flame takes place suddenly; in the lifted lean flame, blowout is preceded by the onset of large-scale axial oscillations of the main flame about its mean position (Figure 5).

The flame events described are controlled by the operating equivalence ratio of the combustor (Figures 5 and 10). The equivalence ratios at which flame events occur are modified by the existence of back-pressure applied at the exit from the combustor (Figures 6 through 9 inclusive). The sensitivity of the event-equivalence ratios to the exit back-pressure depends on the combustor loading, and this sensitivity generally increases with the loading (Figures 8 and 10).

The application of exit back-pressure to the research combustor exerts a favorable influence on the lean blowout (Figure 11). At fixed combustor loading, the effect depends on the combustor length to diameter ratio. When acoustic effects and direct loss of the step recirculation zone (Figure 12) are eliminated through use of an appropriate combustor length, the changes in blowout due to exit blockage are sensitive to combustor loading (Figures 11 and 13). Predictably, they are strongest at high loadings approaching the peak heat release rate condition. At low combustor loadings, the improvement in stability due to blockage is consistent with a more persistent anchored flame (Figures 6 and 7), but conflicts with an earlier onset of large-scale axial movements of the lifted flame (Figure 8).

The presence of the outlet blockage changes the isothermal flow field in the combustor by causing acceleration of the mean axial velocities about the centerline (Figures 3 and 4), and by introducing an additional recirculation zone on the upstream face of the orifice plate placed at the combustor exit. Acceleration of the central flow is evident as close as 125 mm downstream from the step plane (Figure 3), or, at an L/D of 0.83 in the 4.9 L/D combustor at 45.1 percent blockage. This is upstream of the reattachment plane for the step recirculation, which is at about 2.82 L/D (Sturgess et al., 1990). With a free exit in isothermal flow, the central flow is decelerated as the fuel and air jets merge and expand into the combustor around the step recirculation zone. The net acceleration that results with exit blockage represents a modification of the shear layers, and thus, flame holding in these shear layers can be expected to be changed.

The wall static pressure measurements in the step recirculation zone show that combustion suppresses a sensitivity to jet velocity ratio that is apparent in isothermal flow (Figures 19 and 21); the addition of exit blockage in isothermal flow exercises a similar effect (Figure 20).

With combustion, it can be inferred from wall thermocouple measurements that the position of the step recirculation zone reattachment shifts according to the equivalence ratio (Figure 18). For lifted flames, the dependency on equivalence ratio is modified by the degree of outlet blockage (Figure 18). From wall static pressure tap measurements, the size of the orifice plate recirculation is inferred also to be influenced by combustion (Figure 23). For a lifted flame at a given blockage, the movements of these two stagnation planes with equivalence ratio is such that a constant separation between them exists (Figures 24 and 25), i.e., there is no direct interference. When the attached pilot flame condition is established, movement of the step recirculation zone reattachment essentially ceases (Figure 24). However, the orifice recirculation zone continues to decrease in size (Figure 24), with the result that the separation between stagnation planes is increased (Figure 25). Therefore, it is unlikely that the lean blowout improvement with exit blockage is associated with direct modification of the step recirculation zone.

The "quick-look" at mean gas temperature profiles shows the existence of the pilot flame for equivalence ratios when it is present (attached flame), and indicates slightly increased temperatures in the step recirculation zone and on the combustor centerline in the near-field. For lifted flames, exit blockage exerts its greatest effect in the near-field on the combustor centerline, particularly associated with the small, central recirculation bubble; there is little effect in the step recirculation zone. The CARS p.d.f.'s confirm earlier findings by OH emission and TFP measurements that the pilot flame is intermittently present even when direct observations indicate that it is lost and the main flame is lifted.

Fluctuating gas temperatures along the combustor centerline are insensitive to exit blockage (Figure 29); however, they once again confirm the strong dynamic nature of the flow associated with the central recirculation bubble that is generated by entrainment of the central fuel jet by the much stronger surrounding annular air jet (Sturgess et al., 1991b). In the near-field (at 5 mm) the radial profiles of fluctuating temperature suggest that exit blockage is a dampening effect; only slightly in the step recirculation, but much more strongly in the jet shear layers (Figure 30).

Back-pressuring the flame (by exit blockage in this case) exerts a powerful stabilizing effect on lean blowout, especially at the high combustor loadings that can represent critical operating conditions for military aircraft. Direct action of back-pressure on the step recirculation zone does not seem to take place. The back-pressure acts most strongly on the initial processes occurring in the jet shear layers by modifying their trajectories and turbulence characteristics. These initial processes emerge as being critical to the overall flame stabilization, whether the main flame is attached or lifted. Evidence is building (here and in earlier work) that dynamic behavior of the flow in the near-field can control the combustion process, perhaps through radical changes in radial mass transport.

The present results confirm that future attention should be directed at the pilot flame, the circumstances of its existence and its contribution to the main flame. The dynamic interactions of the central recirculation bubble with the jet shear layers and of the jet shear layers with the step recirculation zone must be explored in detail, and characterized if possible. It would be desirable if such future studies could include a mass transport experiment, and time-resolved flow visualization of the combustion in the shear layers.

CONCLUSIONS

1. Back-pressure by means of exit blockage does exert an effect on the lean blowout characteristics of a combustor. The effect is weakest at low combustor loadings near the flammability limits, and strongest at high combustor loadings near the peak heat release rate. Modification of the effect occurs with changes in combustor length to diameter ratio.

2. Direct interference effects of exit blockage on the step recirculation zone do not occur.

3. The major effects of exit blockage on lean blowout are due to changes in the fuel and air jet shear layers, and in the interaction of this shear layer with the step recirculation zone and with the central recirculation bubble. Dynamic processes appear to play a significant part in these interactions.

4. Future experimental work should concentrate on the near-field region, the dynamic interactions taking place there, and the circumstances governing the existence and role of the anchored flame.

5. The combustor exhibits consistent and well-characterized flame behavior that depends on equivalence ratio and exit blockage. The ability to represent this behavior will provide a stringent test of the realism of any numerical modeling (CFD) of this combustor.

ACKNOWLEDGEMENTS

The authors wish to acknowledge the contributions to this work from their colleagues at Wright-Patterson Air Force Base and Pratt & Whitney, and also, from Dr. P. Hedman, Brigham Young University, Provo, Utah. The University of Dayton work was supported by the U.S. Air Force Wright Laboratories, under Contract F33615-87-C-2767 (Contract Monitor Dr. W. M. Roquemore), and Pratt & Whitney was supported under Contract F33615-87-C-2822 (Contract Monitors 1st Lt. A. L. Lesmerises and Mr. D. Shouse). The authors thank the Air Force and Pratt & Whitney for permission to publish the results of this research.

REFERENCES

Chen, T. H., 1991, private communication of unpublished work.

Gupta, A. K., Lilley, D. G., and Syred, N., 1984, Swirl Flows, Abacus Press.

Heneghan, S. P., and Vangsness, M. D., 1990, "Instrument Noise and Weighting Factors in Data Analysis," *Experiments in Fluids*, Vol. 9, pp. 290–294.

Heneghan, S. P., and Vangsness, M. D., 1991, "Analysis of Slit Function Errors in Single-Shot Coherent Anti-Stokes Raman Spectroscopy (CARS) in Practical Combustors," *Reviews of Scientific Instruments*, Vol. 62, pp. 2093–2099.

Heneghan, S. P., Vangsness, M. D., Ballal, D. R., Lesmerises, A. L., and Sturgess, G. J., 1990, "Acoustic Characteristics of a Research Step Combustor," AIAA Paper No. AIAA-90-1851. (to appear in *Journal of Propulsion and Power*).

Heneghan, S. P., Vangsness, M. D., and Pan, J. C., 1991, "Simple Determination of the Slit Function in Single Shot CARS Thermometry," *Journal of Applied Physics*, Vol. 69, pp. 2692–2695.

Lefebvre, A. H., 1983, Gas Turbine Combustion, Hemisphere Publishing Corp., McGraw-Hill Book Company.

Lewis, B., and von Elbe, G., 1961, Combustion, Flames and Explosion of Gases, 2nd Edition, Academic Press.

Morrison, G. L., Tatterson, G. B., and Long, M. W., 1987, "A 3-D Laser Velocimeter Investigation of Turbulent, Incompressible Flow in an Axisymmetric Sudden Expansion," AIAA Paper No. AIAA-87-0119, AIAA 25th Aerospace Sciences Meeting, Reno, Nevada.

Pitz, R. W., and Daily, J. W., 1983, "Combustion in a Turbulent Mixing Layer Formed at a Rearward Facing Step," *AIAA Journal*, Vol. 21, No. 11, pp. 1565–1569.

Roquemore, W. M., Reddy, V. K., Hedman, P. O., Post, M. E., Chen, T. H., Goss, L. P., Trump, D., Vilimpoc, V., and Sturgess, G. J., 1991, "Experimental and Theoretical Studies in a Gas-Fueled Research Combustor," AIAA Paper No. AIAA-91-0639, presented at the 29th Aerospace Sciences Meeting, Reno, Nevada.

Stevenson, W. H., Thompson, H. D., Gold, R. D., and Craig, R. R., 1982, "Laser Velocimeter Measurements in Separated Flow with Combustion," Paper 11.5, presented at the International Symposium of Laser-Doppler Anemometry in Fluid Mechanics, Lisbon, Portugal.

Sturgess, G. J., Sloan, D. G., Lesmerises, A. L., Heneghan, S. P., and Ballal, D. R., 1990, "Design and Development of a Research Combustor for Lean Blowout Studies," ASME Paper 90-GT-143, (to appear in *Transactions of ASME, Journal of Engineering for Gas Turbines and Power*).

Sturgess, G. J., Sloan, D. G., Roquemore, W. M., Reddy, V. K., Shouse, D., Lesmerises, A. L., Ballal, D. R., Heneghan, S. P., Vangsness, M. D., and Hedman, P. O., 1991a, "Flame Stability and Lean Blowout – A Research Program Progress Report," *Proc. 10th ISABE*, Nottingham, England, pp. 372–384.

Sturgess, G. J., Heneghan, S. P., Vangsness, M. D., Ballal, D. R., and Lesmerises, A. L., 1991b, "Isothermal Flow Fields in a Research Combustor for Lean Blowout Studies," ASME Paper 91-GT-37, (to appear in *Transactions of ASME, Journal of Engineering for Gas Turbines and Power*).

Sturgess, G. J., Heneghan, S. P., Vangsness, M. D., Ballal, D. R., and Lesmerises, A. L., 1991c, "Lean Blowout in a Research Combustor at Simulated Low Pressures," ASME Paper 91-GT-359, (to appear in *Transactions of ASME, Journal of Engineering for Gas Turbines and Power*).